 MCB, vol.4, no.4, pp.227-237, 2007

Osmoregulatory Function of Large Vacuoles Found in Notochordal Cells of the Intervertebral Disc Running Title: An Osmoregulatory Vacuole

Christopher J. Hunter[*,†], **Sophia Bianchi**[*], **Phil Cheng**[‡], **Ken Muldrew**[*,‡]

Abstract: The nucleus pulposi of many species contain residual cells from the embryonic notochord, which exhibit a very unusual appearance (large vacuoles occupying ∼80% of the cell volume, surrounded by an actin cytoskeleton). While the vacuoles have been qualitatively described, their composition and function has remained elusive. Given that these cells are believed to generate and experience significant osmotic pressures in both the notochord and intervertebral disc, we hypothesized that the vacuoles may serve as osmoregulatory organelles. Using both experimental and theoretical means, we demonstrated that the vacuoles contain a low-osmolality solution, generated via ion pumps on the vacuolar membrane. During hypotonic stress the vacuoles release their contents into the cytoplasm, diluting the cytoplasm and restoring the osmotic balance across the cell membrane. Thus the vacuoles function to regulate the cell volume and tonicity during rapid osmotic stress, protecting the cells from potentially damaging swelling pressures.

1 Introduction

The intervertebral discs (IVDs) develop from both the embryonic mesenchyme and notochord(1). During embryogenesis, the notochord is surrounded by mesenchymal cells, which synthesize the fibrocartilaginous annulus fibrosus and the osseous vertebral bodies. The notochord virtually disappears in the osseous sites, but persists inside the primitive annulus fibrosus, where it is believed that the entrapped notochord cells synthesize the nucleus pulposus(2, 3). In some species, the notochordal cells persist through most of adult life, while in other species, they gradually disappear during aging, and are replaced by cells which resemble articular cartilage chondrocytes(1, 4). The functional significance of the residual notochordal cells remains to be identified, but some preliminary studies suggest that they may play a role in delaying fibrotic overgrowth of the nucleus and ultimate degeneration of the discs(5, 6).

The notochord undergoes substantial changes in stiffness, geometry, and volume throughout embryogenesis. Adams and coauthors suggested that these changes are at least partly the result of osmotic swelling in the tissue generated by the notochordal cells(7). The embryonic stage is not the only time when the IVD experiences strong osmotic pressures. The IVD undergoes substantial stresses due to motion and axial loading of the spine, generating large hydrostatic pressures in the nucleus, which have been hypothesized to generate large osmotic pressures across the cell membrane(8, 9). However, the plasma membrane can only maintain hydrostatic pressures that are less than 10^{-4} atm (10). Therefore osmotic stress must be generated at a tissue scale, and the cells must be capable of compensating forany osmotic imbalances that occur at the cell scale.

We have previously reported on the three-dimensional organization of cells in the canine nucleus pulposus, in particular identifying large vacuolar structures which were surrounded by a dense actin cortex(11). In that study, we failed to identify the contents of the vacuoles or a containing membrane. In the present study, we identify the structure of the vacuolar membrane and inves-

[*] Corresponding author. Phone: (403) 220-8503 Fax: (403) 282-8406 E-mail: chunter@ucalgary.ca. Department of Mechanical and Manufacturing Engineering, University of Calgary, Calgary, AB T2N 1N4, Canada

[†] Centre for Bioengineering Research and Education, University of Calgary

[‡] Department of Cell Biology and Anatomy, University of Calgary

tigate the behavior of the cells and vacuoles under osmotic stress. We present evidence to show that these vacuoles are newly described mammalian organelles that function as fast-acting osmoregulatory elements within the cells.

2 Materials and Methods

2.1 Notochordal Cell Preparation

Following approval of the animal care committee, lumbar IVDs were collected from 15 young, skeletally mature, mongrel dogs (age <2 years, 20-25 kg) within two hours of euthanasia, yielding 75 discs. The dogs were purpose-bred mongrels from a single breeder using primarily German shepherd and husky stock, and were therefore presumably nonchondrodystrophoid(12). The discs were all categorized as stage 1 on the Bray and Burbidge scale(13), with a gelatinous nucleus pulposus, distinct nuclear-annular demarcation, and normal annular lamellae (approximately equivalent to grade I on the Thompson scale for human IVDs(14)). The lumbar spine was removed *en bloc* and transferred to a cell culture hood, where the IVDs were cut open and the nuclei pulposi were removed and transferred to phosphate-buffered saline (PBS). For cell clusters (osmotic shock and FRAP (fluorescence recovery after photobleaching) experiments), the nuclei were passed twice through an 18G needle to separate cell clusters, then suspended in a thin film of 1% low melting point agarose (Sigma Aldrich, Oakville, ON, Canada) on #1 coverslips to prevent motion of the sample during imaging.

For isolated cells, the nuclei were digested for 90 minutes in 0.4% w/v Pronase (Roche Applied Science, Laval, QC, Canada), 0.004% w/v DNAse II (Sigma Aldrich), followed by an overnight digestion in 0.012 % w/v collagenase type II (Sigma Aldrich), 0.004 w/v DNAse II and 5% fetal bovine serum (FBS). The resulting digest was filtered through a sterile 70 μm nylon mesh filter and washed twice with PBS. The cells were then suspended in Dulbecco's Modified Eagle's Medium (Invitrogen, Burling, ON, Canada).

2.2 V79W Chinese Hamster Fibroblast Cell Sample Preparation

In order to compare notochordal cell response to osmotic stress, a well-characterized control was utilized. V79W Chinese hamster fibroblast cells were grown in culture at 37°C using GIBCO RPMI Medium 1640 (Invitrogen) and 5% FBS/1% penicillin-streptomycin (Invitrogen). To obtain a cell sample, 1 mL of porcine trypsin (Invitrogen) was added to a confluent T75 flask and swirled for approximately one minute to cover the culture surface. RPMI medium (2mL) was then added and the cell suspension was transferred by pipette to a 15 mL centrifuge tube and centrifuged at 163 rcf for 5 min. The pellet was then mixed with 2.5 mL of fresh medium and vortexed to distribute the cells.

2.3 Sample Imaging

Three-dimensional image stacks were collected on a Zeiss LSM 510 confocal laser scanning microscope using either a 25x 0.80NA water-immersion or a 63x 1.40NA oil-immersion objective lens (Carl Zeiss Inc., Toronto, ON, Canada). The laser power setting (488 nm excitation) was adjusted as required for the particular specimen (typically 20-30%). Images were collected as stacks of optical sections (z=10 μm on the 25x objective and z=1 μm on the 63x objective) at 512x512 pixel resolution with 2 line averaging. No further image processing was performed.

For transmission electron microscopy, cells were fixed with 2.5% glutaraldehyde in 0.1M cacodylate buffer (pH 7.4) for 2 hours at room temperature, then washed three times with the same buffer and postfixed with 1% osmium tetroxide in 0.1M cacodylate buffer (pH 7.4) for 1 hour at room temperature. Samples were then dehydrated through a graded alcohol series and embedded in Spurr's resin. Ultrathin sections were cut with a diamond knife, stained with uranyl acetate and lead citrate, and examined on a Hitachi H-7000 electron microscope at 75 kV.

2.3.1 Osmotic Shock

Agarose-embedded cell clusters (1% low melting-point agarose dissolved in isotonic PBS, ∼50 ul per gel) were transferred to the confocal microscope in a bath of 5ml PBS, then imaged at 4 sec/frame over 20 minutes. An isotonic (310 mOsm) bath was used for the first minute, then changed to a hyper- or hypotonic bath for 9 minutes, then changed back to isotonic conditions for the final 10 minutes of imaging. These times were found in pilot experiments to be sufficient to obtain equilibrium in cell diameter. Osmotic shock was applied via the delivery of either a concentrated bolus of sucrose (hypertonic) or pure water (hypotonic) to generate osmolarities of 550, 450, 210, or 31 mOsm. The osmolality of each solution was verified using an osmometer (Osmette A, Precision Systems, Inc.).

2.4 Immunostaining

Agarose-embedded cell clusters were fixed in 4% paraformaldehyde and stained with a monoclonal antibody to pan-alpha sodium/potassium ATPase (Abcam M7-PB-E9, Cambridge, MA, USA), then with a FITC-conjugated anti-mouse IgG secondary (Sigma). The samples were imaged on the confocal microscope, taking 8 μm optical sections.

2.5 Fluorescence Recovery After Photobleaching

In order to determine whether the observed permeabilization was an artifact due to damage or the result of a reversible system, the re-partitioning of calcein had to be tested after hypotonic stress. Therefore the resealing of the vacuole membrane was confirmed using Fluorescence Recovery After Photobleaching (FRAP)(15). It was hypothesized that, if a vacuole remained bleached after restoration to isotonic conditions, then the containing membrane was able to reseal after osmotic shock, while if the vacuole leaked fresh fluorophore into the lumen, then the membrane was compromised by osmotic shock.

Nucleus pulposus tissue from 2 of the animals (4 discs) was prepared and embedded as above, then washed three times in Phosphate Buffered Saline (PBS) and incubated in 2 μM calcein-AM (Invitrogen, Burlington, ON, Canada) for 2 hours. The gels were then washed three times in isotonic PBS (310 mOsm) and transferred to the confocal microscope in a bath of PBS. The inclusions were discharged with a 10 minute osmotic shock at 31 mOsm, and the osmolality was then restored to 310 mOsm. Individual inclusions (n=13) were photobleached with 60-80 pulses of the 488 nm laser operating at 100% power, until the inclusions were just barely visible, i.e., to approximately 35% of original fluorescence. Image fields (10 μm-thick optical slices) were then captured every 4 seconds for 10 minutes to monitor the recovery (Figure 4, inset). These fields were analyzed using Scion Image version Beta 4.0.2 (Scion Corp., Frederick, MD, USA) to measure mean pixel intensity within an inclusion. The mean intensity of a bleached inclusion was normalized to that of an untreated inclusion in the same image field, and the resulting values were compared at the initial time, immediately after bleaching, and after 10 minutes of recovery using paired t-tests.

2.5.1 Cell Volume at 4°C

In order to determine whether cell volume was regulated by an active or passive process, cell volume was measured during cooling to 4°C in isotonic medium. This cooling would inhibit the function of any active ATPase molecules (i.e. ion pumps), thus any change in cell volume would be due to the loss of ATPase functionality.

Cells were placed on 18 mm glass coverslips in a Linkam BCS 196 cryostage (Linkam Scientific Instruments, UK) attached to a light microscope. Stage temperature was lowered at 50°C/min to 4°C and held for 30 min. Individual cells were then photographed at 2 min intervals using a Nikon Coolpix 4500 digital camera (World Precision Instruments 10x 28mm eyepiece adaptor) at 10x objective magnification. Photographs were transferred to a computer and two cell diameter measurements were taken using ImageJ (version 1.31, National Institutes of Health, USA). Pixel diameter was converted to actual size by using 20

μm latex calibration beads (Coulter Corporation, Miami, FL). These diameters were averaged and used to calculate cell volume (assuming a spherical cell), which was normalized to the initial volume.

To study the combined effects of external salt concentration and cooling, cells were placed in a 300 mM sucrose (in distilled water) or DMEM solutions and transferred to a Linkam BCS 196 Cryostage on a light microscope between 18 mm glass coverslips. As the experimental duration was less than 30 minutes, it was assumed that pH would be stable during the experiment without further buffering. The stage temperature was lowered at 50°C/min to 4°C and held for 30 min. Individual cells were photographed and diameters were measured and analyzed as described above (n=35 per condition).

To study the effects of cooling on vacuole permeabilization, canine notochordal cells were again imaged on the confocal microscope. While a single group of cells was held in the focal region, chips of dry ice were placed around the microscope stage to cool the stage to approximately 4°C during imaging. Time-lapse (30 second intervals) images were collected over a period of 700-800 seconds.

2.6 Boyle van't Hoff Relationships

Boyle van't Hoff plots were generated by placing cells in various concentrations of PBS (0.1, 0.2, 0.3, 0.5, 0.75, 1, 2, and 3x isotonic) in a 24-well plate and left to equilibrate for at least 10 minutes. The cells were then examined using an Olympus inverted light microscope and 50 cells were photographed for each concentration. Cell diameters were measured using ImageJ and cell volumes at each concentration of PBS were averaged. The osmolality of each solution was measured using an osmometer (Osmette A, Precision Systems, Inc.). The osmotically inactive cell volume fraction was calculated using the Boyle van't Hoff Relation:

where V is the cell volume, π_0 is the intracellular osmolality, π_e is extracellular osmolality, Vw_o is the isotonic cell water volume, and b is the osmotically inactive cell volume.

2.7 Matlab^{TM} Model

Solute and solvent motion across the cell and vacuole membranes were modeled using a finite difference formulation of the simplified coupled transport equations:

$$\frac{dV}{dt} = -L_p ART\Delta M$$

$$\frac{dN}{dt} = PA\Delta M$$

$$M = \frac{N}{V}$$

Where V is volume (m^3), A is surface area (m^2), R is the universal gas constant (J/mol*K), T is temperature (K), L_p is hydraulic conductivity (m/s*Pa), M is molarity (mol/L), N is moles of solute (mol), and P is solute permeability (m/s)(16). A custom Matlab^{TM} model was developed to model a one-dimensional approximation of a cell, with nine vacuoles exchanging material with one cytoplasmic volume, which in turn exchanged material with one infinite extracellular volume. Finite differences were calculated at intervals of 0.1 s over a 10-30 minute period, during which the extracellular solution could be rapidly changed. The vacuole and plasma membranes were assumed to be identical, except for a ratio difference in their ion permeability and hydraulic conductivity. Most of the equation parameters could be estimated directly from experimental data or from the literature. For the remaining parameters (vacuole and cell membrane ion permeability and hydraulic conductivity), experimental cell volumes were fit to the equations using the least-squared difference method to the cooling data. The final set of equations was then run in different bath conditions to simulate hypotonic stress, with the vacuole membranes set to become more permeable (by a factor of 100) at an experimentally determined membrane stretch of 49.6% by area.

2.8 Data Analysis

Data were analyzed using two-tailed t-tests for statistical significance.

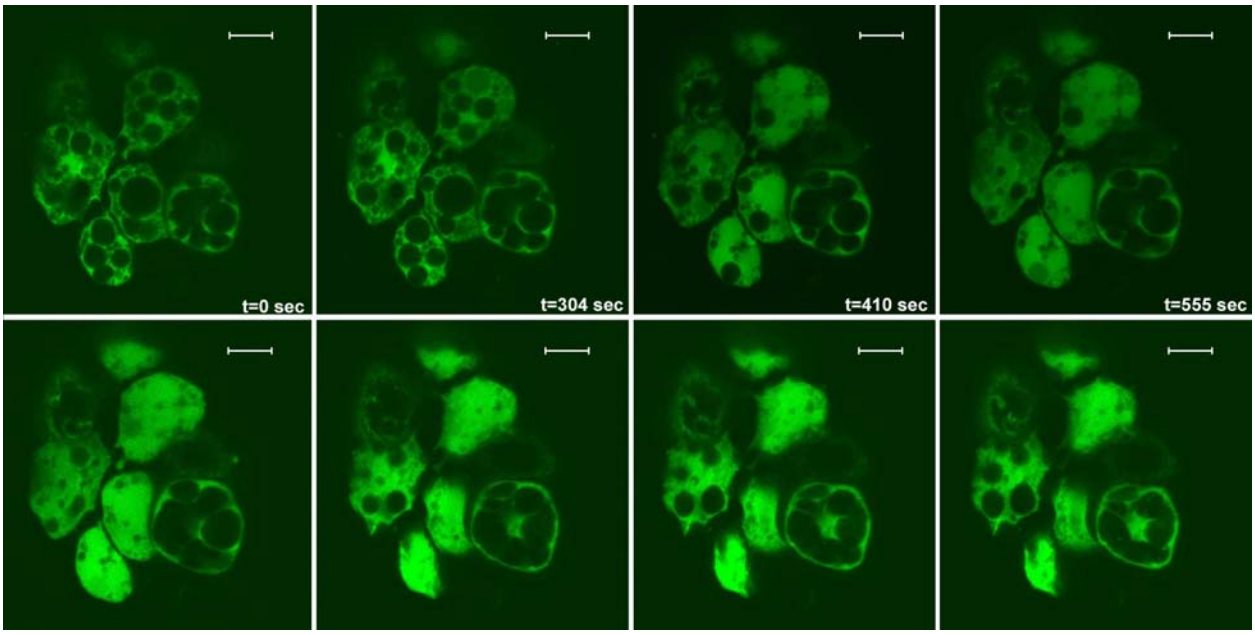

Figure 1: The large vacuoles within notochordal cells become permeable to calcein during hypotonic (31 mOsm) stress (top row), and do not expel the calcein upon restoration to isotonic (310 mOsm) conditions (bottom row). Five cells from agarose-embedded cell clusters are visible in this field; 1-μm optical sections, scale bar 20 μm. Time points are matched in both the "stressed" and "restored" rows.

3 results

3.1 Osmotic Shock

Staining with calcein-AM resulted in an even distribution of fluorophore throughout the cytoplasm, but with complete exclusion of fluorophore from the vacuole lumen, suggesting a membrane structure which could exclude large molecules (Figure 1, first panel). In isotonic conditions, this state would remain for at least several hours (the longest duration examined).

At the 550, 450, and 210 mOsm conditions, the cells behaved as osmometers: hypertonic stress resulted in cell shrinkage, while hypotonic stress resulted in cell swelling. No other effects were observed at these levels of osmotic stress. At the extreme stress state of 31 mOsm, however, the vacuoles were observed to become rapidly filled with fluorescent dye, generally in less than one frame (4 seconds) (Figure 1, top row). Restoring the bath to isotonic conditions did not reverse the dye compartmentalization, but did result in some out-of-plane motion of vacuoles (Figure 1, bottom row). It was presumed that the plasma membrane was intact during osmotic stress, as calcein was not observed to leak out of the cells for up to 30 minutes after the application of shock (not shown).

Cell volume appeared to be dependent upon vacuole permeability. Prior to the permeabilization event, cells in hypotonic conditions continually swelled; however, after the permeabilization of the vacuoles, the cells began to shrink back towards their initial volume and continuing to approximately 90% of initial diameter (Figure 2). The cells tested had a typical roundness coefficient (4πArea/Perimeter^2) of >0.95 with a worst case of 0.75. Since the cells appeared to shrink and swell isotropically, the spherical assumption is reasonable.

The permeabilization event was likewise seen during cell cooling, approximately 570 seconds after the application of the dry ice chips to the stage (not shown).

3.2 Immunostaining

Alpha sodium/potassium ATPase was detected both on the cell surface and the interior of the

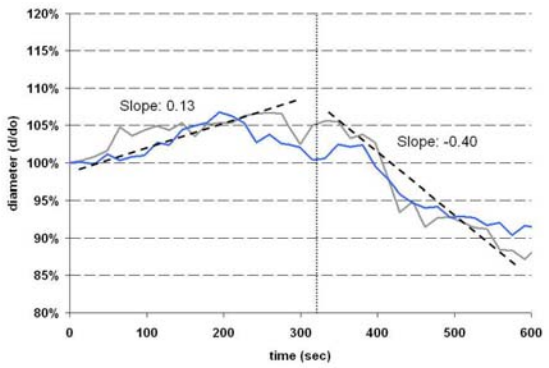

Figure 2: Cell diameter during hypotonic stress for two representative cells. Cells swelled continuously until the vacuoles began to "permeabilize" (first uptake of calcein into the vacuoles; vertical dashed line), at which point the cells began to shrink back towards initial volume.

cells, indicating the presence of ion pumps on the vacuoles (Figure 3).

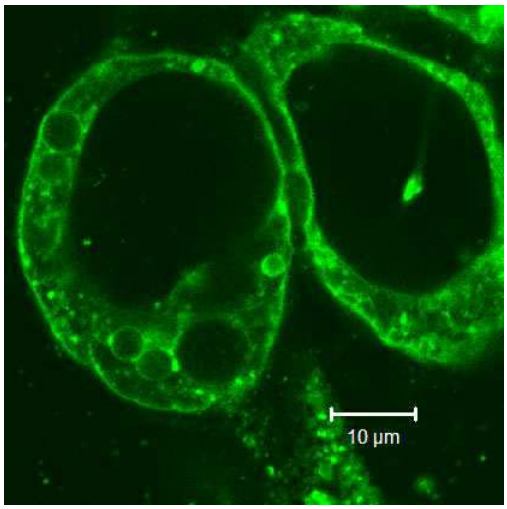

Figure 3: Results of pan-sodium/potassium ATPase immunostaining. Scale bar μm.

3.3 *Fluorescence Recovery After Photobleaching*

Osmotic shock resulted in a flooding of the vacuole lumen with fluorophore, as before. While at hypotonic conditions, the vacuole could not be bleached by any duration of laser exposure (not shown), suggesting that the vacuoles were held in a permeable state under hypotonic stress. Similarly, it was not possible to significantly bleach a region of the extravacuolar cytosol under any osmotic state (not shown). If the cells were returned to isotonic conditions, the vacuole could be bleached by 60-80 pulses of the laser, and remained bleached for at least 10 minutes afterwards (Figure 4, Figure 5).

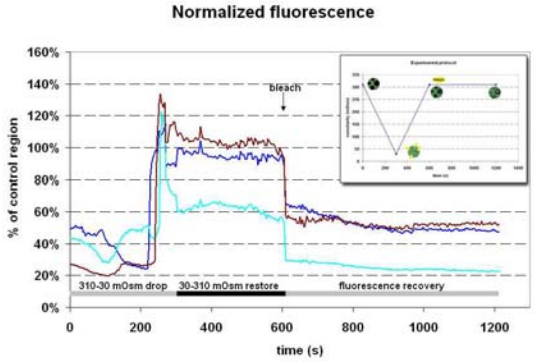

Figure 4: Results of FRAP studies; three representative traces indicate that photobleached vacuoles remain bleached for at least 10 minutes after restoration to isotonic conditions. Inset: experimental protocol for FRAP studies.

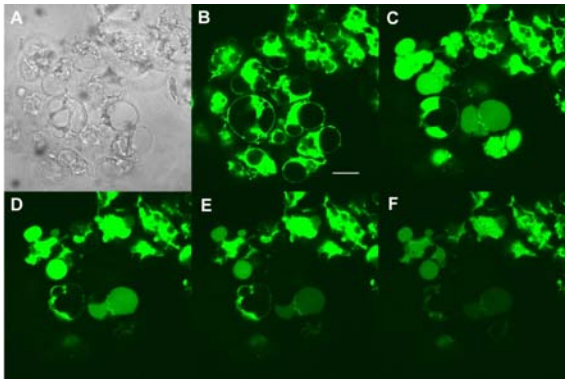

Figure 5: Results of FRAP studies; (A) initial state, DIC optics; (B) initial state, fluorescence optics; (C) under hypotonic conditions (31 mOsm); (D) returned to isotonic conditions; (E) after bleaching of select vacuoles; (F) after 10 minutes of recovery at isotonic conditions. Scale bar 20 μm.

3.4 Transmission Electron Microscopy

Examination of the cells with TEM revealed a fine multilayered membrane around the vacuoles, containing from one to five layers (Figure 5). The membranes were generally not visible around the entire vacuole, but rather appeared as periodic fragments, suggesting that the membranes were susceptible to disruption during fixation and preparation.

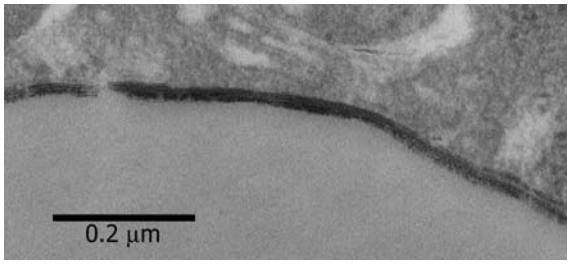

Figure 6: TEM of the multilayered vacuole membrane. Scale bar 200 nm.

3.5 Cell Volume at 4°C

At 4C, the cell cannot metabolically maintain the low Na+ concentration in the cytoplasm. Na+ leaks into the cells passively causing water to follow osmotically. Both the V79W cells and the canine notochordal cells swelled over the 30 minutes at 4 °C, however the notochordal cells exhibited a substantially larger swelling which reached an equilibrium 10 minutes after cooling. The notochordal cells swelled to 132% of their initial volume after 8 minutes and remained enlarged at approximately 125% of initial volume for 20 minutes when they decreased slightly in volume to just less than 120%. The V79W cells swelled to 111% of initial volume by 14 minutes at which point cell volume declined steadily to 105% after 30 minutes (Figure 7).

The notochordal cell volume in 300 mM sucrose solution at 4°C exhibited a slight increase over the 30 minutes. Cell volume started at 110% of initial volume (initial volume was measured at room temperature, but already equilibrated in sucrose), rose approximately 10% after 8 min and remained constant until the end of 30 minutes. The average cell volume at room temperature and isotonic conditions for canine notochordal cells in DMEM was found to be approximately 7180<9190<12400 μm^3 (mean bracketed by 95% confidence intervals based on a lognormal distribution). When placed in the 300 mM sucrose solution, the average notochordal cell volume decreased by more than half to approximately 3130<3970<5310 μm^3 (mean bracketed by 95% intervals). The means were significantly different ($p<0.001$) on a t-test of the logarithmically transformed data.

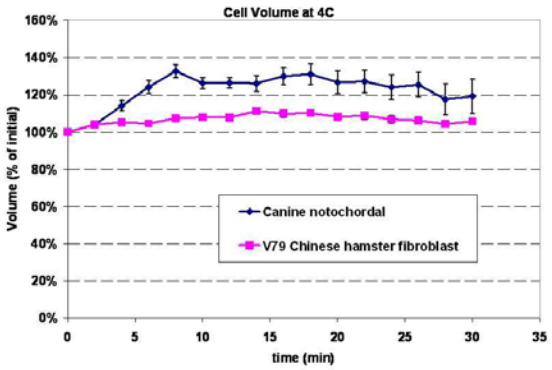

Figure 7: Cell volume during an extended hold at 4°C. The notochordal cells swelled significantly more than V79 fibroblasts (n=35 per condition).

3.6 Boyle van't Hoff Plot

The Boyle van't Hoff plot for the canine notochordal cells shows a point of inflection apparently at isotonic osmolality (Figure 8a), while the plot for the V79W Chinese hamster fibroblast cells was linear with a y-intercept of 0.16 (Figure 8b). For the notochordal cells, the osmotically inactive cell volume fractions in hypertonic and hypotonic conditions were 0.83 and 0.05, respectively.

From the Boyle van't Hoff plot, a relative cell volume of 1.3 times isotonic corresponds to a 0.5X dilution factor. The intracellular concentration is therefore half of normal, or 150 mM. If we consider that 80% of the notochordal cell volume consists of these inclusion vacuoles, then it is possible to calculate an approximate concentration of the solution contained within the vacuoles:

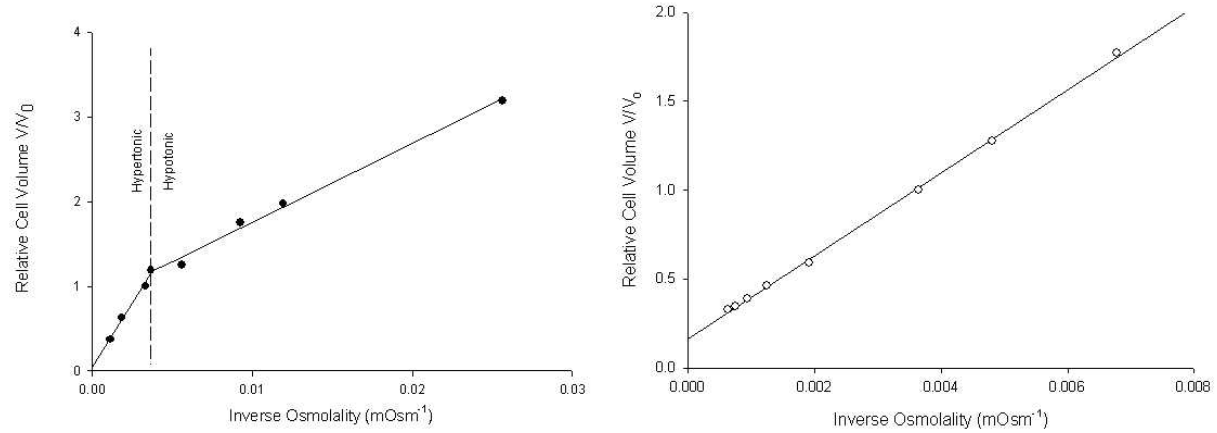

Figure 8: Boyle van't Hoff plots for notochordal cells (left) and V79 fibroblasts (right). Note the inflection point at isotonicity for the notochordal cells, while the graph is a straight line for V79 fibroblasts (n=50 per condition).

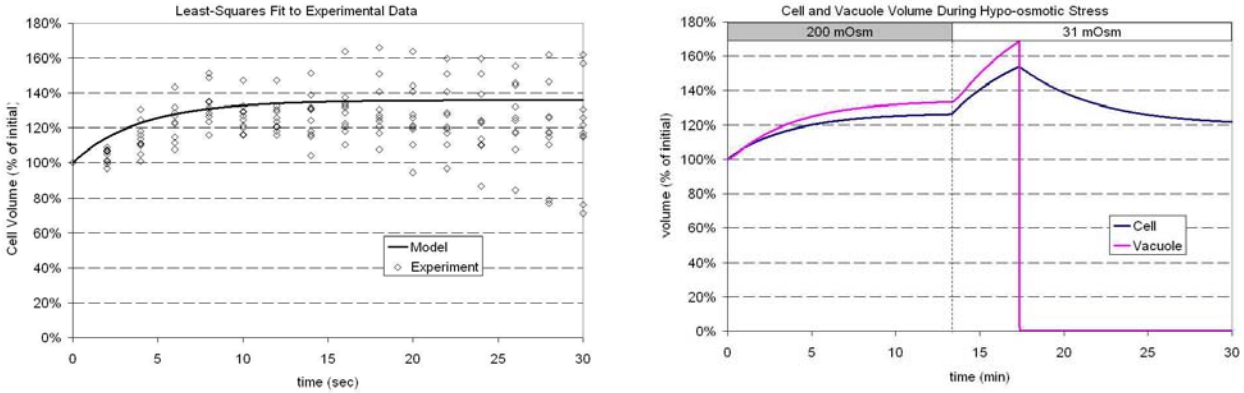

Figure 9: Matlab model results, least-squares regression to data (left) and prediction of experimental "permeabilizing" of the vacuoles (right).

(Vacuolar fraction of cell volume) × (vacuole concentration)
+ (cytoplasmic volume fraction) × (cytoplasm concentration) = 150 mM

Plugging in the above values give a vacuole solute concentration of 112.5 mM.

3.7 Matlab™ Model

Based upon the above experimental data, the vacuoles were assumed to contain cytoplasm diluted to obtain a vacuole osmolality of 112 mOsm. Cell swelling data were successfully fit to the model, with an r^2 value of 0.99 (Figure 8). The fit yielded an estimated vacuole permeability of 0.25 times that of the plasma membrane (both hydraulic and ion), and a plasma membrane hydraulic conductivity of $1.1\text{x}10^{-13}$ m/s•Pa. In hypertonic (450 mOsm) conditions, the model cells and vacuoles both shrank by 40% volume (not shown), while in mild hypotonic (200 mOsm) conditions, the model cells and vacuoles both swelled by 40% volume (Figure 8). When a strong hypotonic shock (31 mOsm) was delivered, the cells and vacuoles swelled for several minutes, then the vacuole membrane stretch reached the critical value, causing the membrane permeability to decrease, and the cells and vacuoles suddenly shrank back towards baseline conditions (Figure 8).

4 Discussion

At this point, a change of terminology appears to be in order. While these structures were previously referred to by ourselves and others as "vacuoles" (defined in MeSH as "any spaces or cavities within a cell. They may function in digestion, storage, secretion, or excretion"), the present evidence justifies the more specific term "vesicles" (cytoplasmic vesicles are defined in MeSH as "membrane-limited structures derived from the plasma membrane or various intracellular membranes which function in storage, transport or metabolism").

Calcein-AM is membrane permeant and does not fluoresce until it is cleaved by esterases, which are abundant in the cytoplasm, at which point it becomes membrane impermeant and fluoresces green. The results shown here suggest that calcein enters into the cytoplasm of notochordal cells, and then cannot pass across the vacuolar membrane until it is permeabilized by a stress-related mechanism.

These results suggest a unique osmotic response mechanism in canine notochordal cells. The temporary and reversible permeabilization of the osmoregulatory vesicles allowed calcein to flow in. This "discharging" of the osmoregulatory vesicles appeared to occur in response to cell swelling or related factors, and appeared to play a role in regulating cell volume. The results of the FRAP experiments demonstrated that the vesicles were held "open" at hypotonic conditions, but were able to close upon return to isotonic conditions.

TEM revealed an unusual structure to the vesicle membrane, with up to five distinct layers. These multiple layers are likely important in the "discharging" process, but the mechanism has yet to be revealed. Further studies will be required to examine the ultrastructure of the vesicles and how they may function during osmotic stress.

The results from the cell cooling experiments and the computational model suggest that an active mechanism is working to maintain a hypotonic solution in the vesicles. A high density of ion pumps on the vesicular membrane is likely generating this low-osmolality solution inside the vesicle. Under hypotonic stress, the low-osmolality solution in the vesicles is released, diluting the cytoplasm and thereby relieving the cell from osmotic stress. When the cells are cooled to 4°C, the ion pumps do not function and the osmolality of the vesicles increases along with the cytoplasm, causing the cells to swell and the vesicles to discharge as observed.

The non-linear Boyle van't Hoff plot further suggests that an active volume regulation is taking place in the form of a rectified flow of water and ions. For notochordal cells, the plot indicates an osmotically inactive cell volume fraction of 83% in a hypertonic environment, while in hypotonic conditions the osmotically inactive volume fraction is 5%. Most mammalian cells follow a linear Boyle van't Hoff relation (within the limits of dilution/concentration of 2-3 times isotonic) with an osmotically active cell volume fraction that is close to the solid fraction of the cell plus the water of hydration(17). The value of 16% osmotically inactive volume seen with V79w fibroblasts is typical. These data suggest a unidirectional flow of water and ions across the vesicle membrane, and a singular responsiveness to hypotonic stress.

The hydrostatic pressure gradient that would presumably develop as a result of this osmotic pressure gradient is probably dissipated through membrane permeability to water before it gets large enough to rupture the membrane. It should be remembered that standard EM fixation techniques involve osmotic events (e.g. as with the addition of glutaraldehyde) that may have resulted in the fragmentation of the vesicle membrane before fixation occured.

The direct mechanism of release of the vesicular contents may not be cell swelling; from the results of the experiment where notochordal cells were placed in a 300 mM sucrose solution it is evident that the trigger for release is instead a low extracellular sodium chloride concentration. The osmolality of the 300 mM sucrose solution is isotonic, therefore cell volume should remain constant unless the cells are able to detect the absence of sodium chloride. The average notochordal cell volume in sucrose decreased by more than half,

which can be explained by an immediate release of vesicular contents to compensate for the hypo-osmotic stress. This suggests that the vesicles respond to electrolyte concentration, not to osmotic pressure; this explains the abrupt volume loss as the vesicles release their contents, dilute the cytoplasm, and water flows out of the cell down its concentration gradient. Further evidence that the vesicles have discharged comes from the results of the notochordal cells in sucrose at 4°C for 30 minutes. Notochordal cell swelling over the 30 minutes was minimal, likely because the vesicles had already released their contents to dilute the cytoplasm and shrink the cells. The vesicles apparently do not recover at 4°C because active pumping is slowed and therefore cell volume remains constant. Further experiments to determine the threshold for vesicle release and how large the pores are will be useful, in conjunction with further investigation into the biochemical and structural composition of these vesicles.

It is interesting to note that the structure and behavior of the notochordal cells bears little resemblance to any other mammalian cells; the closest analogues appear to be the "giant vesicles" of some frog bladder cells(18), the "contractile vesicles" of certain unicellular organisms(19), and the osmoregulatory vesicles in certain salt-tolerant plants (i.e. mangrove)(20). While an absence of evidence is insufficient to conclude uniqueness, it is certainly intriguing to consider the possibility that these observations mark an entirely new osmoregulatory organelle in a mammalian cell.

The results obtained from this study pose more questions regarding the osmoregulatory function of notochordal cells and their vesicles. For example, they may be residual structures, left over from the embryonic straightening and stiffening of the notochord(21). Alternatively, it is known that diurnal changes in mechanical loading of the spine may induce substantial osmotic stresses in the nucleus pulposus(22, 23). It may be that the vesicles serve to protect the cells from this stress. Further experimentation will be necessary to determine why these cells possess the ability to maintain cell volume under hypo-osmotic stress and how this unique behavior relates to the notochordal cell's role in maintenance of IVD tissue. Answers to these questions may shed more light on the role played by notochordal cells in IVD development, degeneration and repair.

Acknowledgement: Dr. Hunter is an Alberta Heritage Foundation for Medical Research Scholar and an Alberta Ingenuity Fund New Faculty. Ms. Bianchi was supported by the Markin-Flanagan program at the University of Calgary. Many thanks to Dr. Matthias Amrheim and Dr. Wei-Xiang Dong for their assistance with TEM, and to Dr. John Matyas for consultation and technical assistance.

Reference

1. Walmsley, R. (1953): *Edinburgh Med. J.* **60**, 341-363.

2. Bell, G. R. (1996): in *The Lumbar Spine*, eds. Wiesel, S. W., Weinstein, J. N., Herkowitz, H. N., Dvorak, J., & Bell, G. R. (W.B. Saunders Company, Philadelphia, PA), pp. 43-52.

3. Horwitz, T. (1977): *The human notochord: a study of its development and regression, variations, and pathologic derivative, chordoma* (Horwitz, Indianapolis).

4. Trout, J. J., Buckwalter, J. A., & Moore, K. C. (1982): *Anat. Rec.* **204**, 307-314.

5. Butler, W. F. & Fujioka, T. (1972): *Anat Anz* **132**, 465-475.

6. Butler, W. F. (1989): in *The biology of the intervertebral disc*, ed. Gosh, P. (CRC Press, Boca Raton), pp. 84-108.

7. Adams, D. S., Keller, R., & Koehl, M. A. R. (1990): *Development* **110**, 115-130.

8. Urban, J. P. (2002): *Biochem. Soc. Trans.* **30**, 858-864.

9. Urban, J. P. G., Roberts, S., & Ralphs, J. R. (2000): *American Zoologist* **40**, 53-61.

10. Jain, M. (1972): *The biomolecular lipid membrane: A system* (Litton Educational Publishing, Inc..

11. Hunter, C. J., Matyas, J. R., & Duncan, N. A. (2003): *J. Anat.* **202**, 279-292.

12. Hansen, H. J. (1952): *Acta Orthop Scand* **Suppl. 11**.

13. Bray, J. P. & Burbidge, H. M. (1998): *J. Am. Anim Hosp. Assoc.* **34**, 135-144.

14. Thompson, J. P., Pearce, R. H., Schechter, M. T., Adams, M. E., Tsang, I. K., & Bishop, P. B. (1990): *Spine* **15**, 411-415.

15. Wade, M. H., Trosko, J. E., & Schindler, M. (1986): *Science* **232**, 525-528.

16. Kedem, O. & Katchalsky, A. (1958): *Biochim. Biophys. Acta* **27**, 229-246.

17. Dick, D. A. T. (1966): *Cell Water* (Butterworths, Washington).

18. Iwamoto, M., Allen, R. D., & Naitoh, Y. (2003): *J Exp Biol* **206**, 4467-4473.

19. Gronlien, H. K., Stock, C., Aihara, M. S., Allen, R. D., & Naitoh, Y. (2002): *J Exp Biol* **205**, 3261-3270.

20. Mimura, T., Kura-Hotta, M., Tsujimura, T., Ohnishi, M., Miura, M., Okazaki, Y., Mimura, M., Maeshima, M., & Washitani-Nemoto, S. (2003): *Planta* **216**, 397-402.

21. Adams, D. S., Keller, R., & Koehl, M. A. R. (1990): *Development* **110**, 115-130.

22. Urban, J. P. (2002): *Biochem. Soc. Trans.* **30**, 858-864.

23. Urban, J. P. G., Roberts, S., & Ralphs, J. R. (2000): *American Zoologist* **40**, 53-61.